

T. Madura<sup>1,†</sup>; T. Gull<sup>1</sup>; M. Corcoran<sup>1,2</sup>; A. Okazaki<sup>3</sup>; S. Owocki<sup>4</sup>; C. Russell<sup>5</sup>; K. Hamaguchi<sup>1,5</sup>; N. Clementel<sup>6</sup>; J. Groh<sup>7</sup>; D. J. Hillier<sup>8</sup>

<sup>1</sup>NASA GSFC, USA; <sup>2</sup>CRESST & USRA, USA; <sup>3</sup>Hokkai-Gakuen Univ., Japan; <sup>4</sup>Univ. of Delaware, USA; <sup>5</sup>Univ. of Maryland, Baltimore County, USA; <sup>6</sup>Leiden Univ., Netherlands; <sup>7</sup>Geneva Observatory, Switzerland; <sup>8</sup>Univ. of Pittsburgh, USA  
<sup>†</sup>Fellow, NASA Postdoctoral Program, administered by Oak Ridge Associated Universities, Email: thomas.l.madura@nasa.gov

## Abstract

At the heart of  $\eta$  Carinae's spectacular "Homunculus" nebula lies an extremely luminous ( $L_{\text{Total}} \approx 5 \times 10^6 L_{\odot}$ ) colliding wind binary with a highly eccentric ( $e \sim 0.9$ ), 5.54-year orbit (Figure 1). The primary of the system, a Luminous Blue Variable (LBV), is our closest ( $D \sim 2.3$  kpc) and best example of a pre-hypernova or pre-gamma ray burst environment. The remarkably consistent and periodic *RXTE* X-ray light curve surprisingly showed a major change during the system's last periastron in 2009, with the X-ray minimum being  $\sim 50\%$  shorter than the minima of the previous two cycles<sup>1</sup>. Between 1998 and 2011, the strengths of various broad stellar wind emission lines (e.g. H $\alpha$ , Fe II) in line-of-sight (Lo.S.) also decreased by factors of 1.5–3 relative to the continuum<sup>2</sup>. The current interpretation for these changes is that they are due to a gradual factor of 2–4 drop in the primary's mass-loss rate over the last  $\sim 15$  years<sup>1,2</sup>. However, while a secular change is seen for a direct view of the central source, little to no change is seen in profiles at high stellar latitudes or reflected off of the dense, circumbinary material known as the "Weigelt blobs"<sup>2,3</sup>. Moreover, model spectra generated with CMFGEN predict that a factor of 2–4 drop in the primary's mass-loss rate should lead to huge changes in the observed spectrum, which thus far have not been seen. Here we present results from large- ( $\pm 1620$  AU) and small- ( $\pm 162$  AU) domain, full 3D smoothed particle hydrodynamics (SPH) simulations of  $\eta$  Car's massive binary colliding winds for three different primary-star mass-loss rates (2.4, 4.8, and  $8.5 \times 10^{-4} M_{\odot}/\text{yr}$ ). The goal is to investigate how the mass-loss rate affects the 3D geometry and dynamics of  $\eta$  Car's optically-thick wind and spatially-extended wind-wind collision (WWC) regions, both of which are known sources of observed X-ray, optical, UV, and near-IR emission and absorption. We use two domain sizes in order to better understand how the primary's mass-loss rate influences the various observables that form at different length scales. The 3D simulations provide information important for helping constrain  $\eta$  Car's recent mass-loss history and future state.

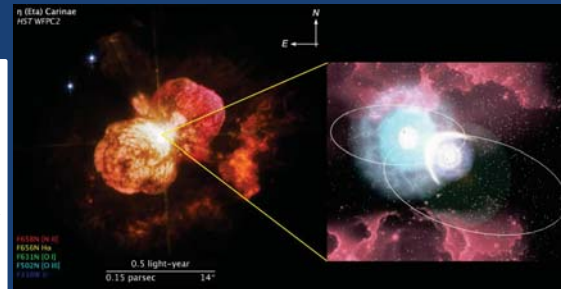


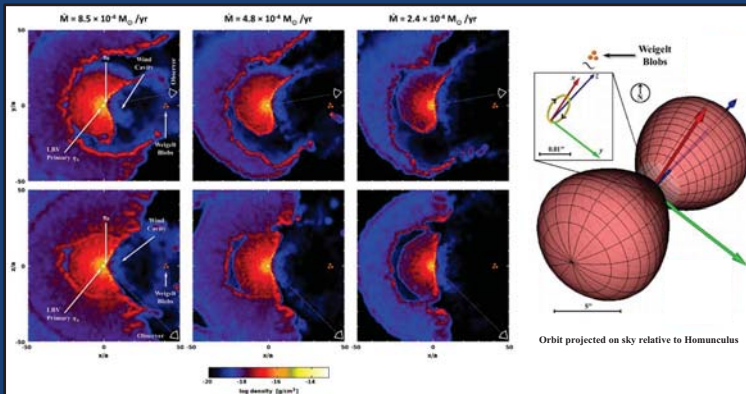
Figure 1: Recent *HST* image of  $\eta$  Carinae (left, NASA, ESA, and the Hubble SM4 ERO Team) with artist's conception (right, A. Damineli, www.etaarinae.iag.usp.br) of the central colliding wind binary.

## The 3D SPH Simulations

We use an improved version of the 3D SPH code in [4, 5]. Radiative cooling and radiative forces, including inhibition, are now implemented. The stellar winds are parameterized using the standard beta-velocity law  $v(r) = v_{\infty}(1 - R_*/r)^{\beta}$ , with  $\beta = 1$ ,  $v_{\infty}$  the wind terminal speed, and  $R_*$  the stellar radius. The binary orbit is set in the  $xy$  plane, with the origin at the system center-of-mass and the orbital major axis along the  $x$ -axis. The outer simulation boundary is set at either  $r = \pm 10a$  or  $r = \pm 100a$ . The adopted model parameters (Table 1) are consistent with those derived from the observations. By convention,  $\phi = 0, 1, 2, \dots$  is defined as periastron and  $\phi = 0.5, 1.5, 2.5, \dots$  apastron.

Table 1: 3D SPH Simulation Parameters	LBV Primary Star	Companion Star
Mass ( $M_{\odot}$ )	90	30
Radius ( $R_{\odot}$ )	60	30
Mass-loss Rate ( $10^{-4} M_{\odot}/\text{yr}$ )	8.5, 4.8, & 2.4	0.14
Wind Terminal Speed (km/s)	420	3000
Wind Momentum Ratio $\eta$	0.12, 0.21, & 0.42	
Orbital Eccentricity $e$	0.9	
Orbital Period	2024 days	
Semimajor axis length $a$	15.45 AU	

Figure 2 (right): Top row: Slices from the 3D simulations at a phase near apastron showing log density in the orbital  $xy$  plane for 3 assumed primary mass-loss rates. The stars, WWC cavity, and Weigelt blobs are marked. The dashed line and eye show the observer's projected Lo.S. Axis tick marks correspond to an increment of  $10a = 154$  AU =  $0.07''$ . Bottom row: Same as top row, but in the  $xz$  plane. Far right panel: Illustration of  $\eta$  Car's orbit (upper left inset, yellow) on the sky relative to the Homunculus for the binary orientation derived by Madura et al. (2012) ( $i = 138^{\circ}$ ,  $\omega = 263^{\circ}$ , and  $PA_s = 317^{\circ}$ ). The red, green, and blue arrows indicate the orbital major (+x), minor (+y), and angular-momentum (+z) axes, respectively. North is up.



## The Spatially-Extended, Time-Variable Interacting Wind Structures

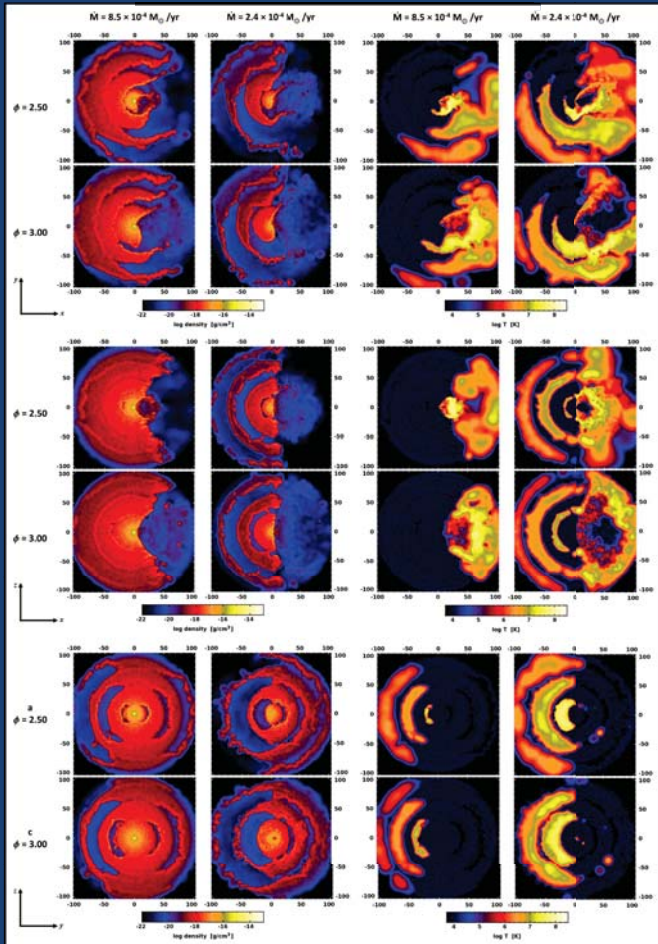


Figure 3: Slices showing log density (left two columns) and log temperature (right two columns) at apastron ( $\phi = 2.5$ ) and periastron ( $\phi = 3.0$ ) in the  $xy$  (top two rows),  $xz$  (middle two rows), and  $yz$  (bottom two rows) planes taken from the  $r = \pm 100a$  3D SPH simulations of  $\eta$  Car assuming primary mass-loss rates of  $8.5 \times 10^{-4} M_{\odot}/\text{yr}$  and  $2.4 \times 10^{-4} M_{\odot}/\text{yr}$  (columns).

## Collapse of the Inner Wind-Wind Collision Zone During Periastron Passage

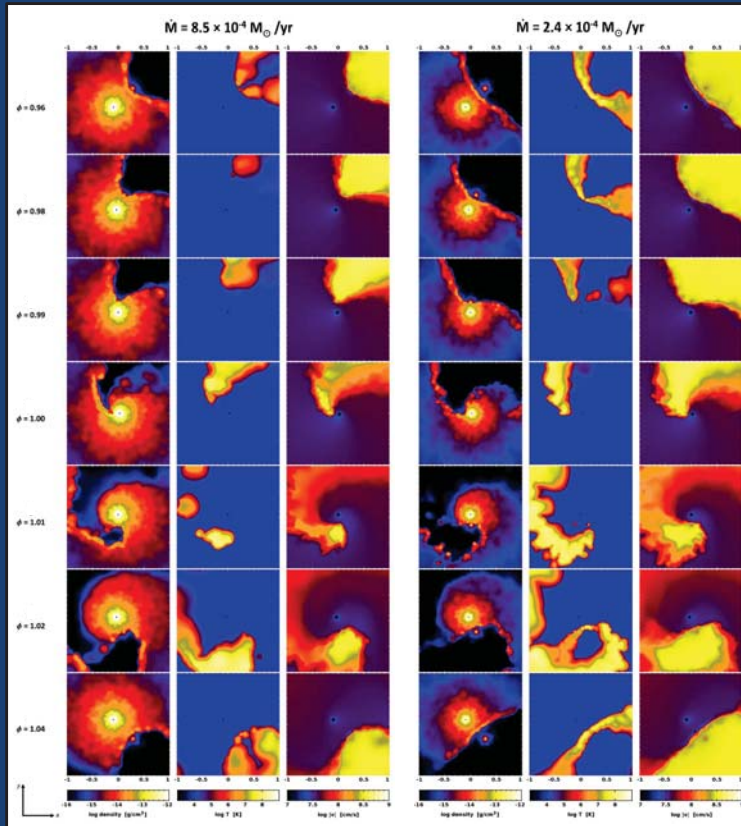


Figure 4: Slices showing density, temperature, and wind speed on a logarithmic scale (columns, left to right, cgs units) in the orbital  $xy$  plane at seven phases around periastron (rows) taken from the  $r = \pm 10a$  SPH simulations of  $\eta$  Car assuming primary mass-loss rates of  $8.5 \times 10^{-4} M_{\odot}/\text{yr}$  (left three columns) and  $2.4 \times 10^{-4} M_{\odot}/\text{yr}$  (right three columns). All plots show the inner  $\pm 1a$  region. Axis tick marks correspond to an increment of  $0.1a \approx 1.55$  AU. The orbital motion of the stars is counterclockwise. The LBV primary is to the left and the companion to the right at apastron. In each simulation there is a "collapse" of the WWC zone between the stars. The hottest gas near the WWC apex vanishes during this time. The higher the primary mass-loss rate, the sooner the collapse occurs before periastron, and the later the recovery of the hot gas after periastron. The collapse appears to be due to the increased effectiveness of radiative cooling in the post-shock wind of the companion at phases around periastron.

### References:

- [1] Corcoran, M. F., et al. 2010, *Apl*, 725, 1528
- [2] Mehner, A., et al. 2012, *Apl*, 751, 73
- [3] Gull, T. R., et al. 2009, *MNRAS*, 396, 1308
- [4] Okazaki, A.T., et al. 2008, *MNRAS*, 388, L39
- [5] Madura, T. L., et al. 2012, *MNRAS*, 420, 2064